

# INFLUENCE OF THE Co:Ni RATIO ON THE PROPERTIES OF Co-Ni NANOPARTICLES AND THEIR CARBON-CONTAINING NANOCOMPOSITES

I.N. Markova<sup>1</sup>, I.Z. Zahariev<sup>1</sup>, M.T. Georgieva<sup>2</sup>, D. Tzankov<sup>2</sup>, D.I. Ivanova<sup>1</sup>,  
M.B. Piskin<sup>3</sup> and L.B. Fachikov<sup>1</sup>

<sup>1</sup>University of Chemical Technology and Metallurgy, 8 Kliment Ohridski blvd., 1756 Sofia, Bulgaria

<sup>2</sup>University of Sofia, Department of Physics, Sofia 1164, Bulgaria

<sup>3</sup>Yildiz Technical University, Davutpasa kampusu A 1003-1004 Esenler, Istanbul, Turkey

Received: January 16, 2017

**Abstract.** Co-Ni nanoparticles are synthesized through a chemical borohydride reduction with 0.2M NaBH<sub>4</sub> in a mixture of water solutions of the chloride salts (0.1M CoCl<sub>2</sub>·6H<sub>2</sub>O and 0.1M NiCl<sub>2</sub>·6H<sub>2</sub>O) at a different Co: Ni ratio at room temperature in open lab space. Template synthesis of the same nanoparticles is carried out using graphite as a support in the presence of β-cyclodextrin yielding carbon-containing nanocomposites. In the both cases of the synthesis it is experimented three ratios of Co: Ni=1:1, 4:1 and 1:4 to study the properties of these nanomaterials in connection with the influence of the different Co and Ni content. The morphology, the elemental, and phase composition are investigated by the help of Scanning electron microscopy (SEM), Energy dispersive spectroscopy (EDS) and X-ray diffraction (XRD) analyses, respectively. Magnetic properties are also examined by the Vibrating Sample Magnetometer (VSM) at room temperature. In the all cases the particle morphology presents assemblies in size from 0.5 to 100 μm formed by nanopartilces due to the unsaturated nanosurface and magnetic forces. The Co-Ni nanoparticles are amorphous in structure. The different ratio of Co: Ni influences the Co and Ni content that is proved by the EDS analysis. The phases formed during the synthesis are also changed depending on the Co: Ni ratio. Co-Ni nanoparticles synthesized at Co: Ni=1:1 and 4:1 ratio have a soft ferromagnetic behavior. On the basis of the Saturation magnetization, Ms [emu/g], the Co-Ni nanoparticles obtained at a ratio Co:Ni=1:1 and 4:1 have better magnetic characteristics than that in the case of a ratio Co:Ni=1:4 and also when graphite is used as a support in the presence of β-cyclodextrin. These Co-Ni nanoparticle powders (Co:Ni=1:1 and 4:1) reveal a good ferromagnetic behavior, which would be suitable for biomedical applications as diagnostic tools and smart treatment agents in cancer and other diseases.

## 1. INTRODUCTION

The preparation and magnetic properties of Co, Ni and Co-Ni nanoparticles obtained by a chemical method are particularly important for biomedicine [1-16]. The magnetic properties of these nanoparticles offer exciting opportunities for delivering drugs to targeted areas in the body replacing radioactive tracer materials, improving the quality of magnetic resonance imaging and

producing smaller data storage devices [3]. By modifying the surfaces of the particles they can avoid the rapid uptake by reticuloendothelial system and prolong their blood circulation time [3,9].

The particle size control and size dispersion require careful control of the nucleation and growth steps in the process and elimination of aggregation during growth. Magnetic Co, Ni, and Co-Ni nanoparticles coated with a polymer layer were found to be stable under ambient conditions without

Corresponding author: I.N. Markova, e-mail: vania@uctm.edu

undergoing oxidation. The saturation magnetization values could be changed significantly by the polymer coating that also determines the final size stability of the coated biocompatible nanoparticles. The magnetic nanosized Co-Ni particles with a modified surface have no harmful effect on biological tissue.

Nanoparticles and nanowires of iron group metals (Fe, Co, Ni) are attractive not only as magnetic materials with the magnetic shape anisotropy, but also for applications to catalytic materials [7,9]. Numerous methods for synthesis of iron group nanomaterials have been reported such as template-assisted electrodeposition, organometallic routes, polyol reduction, and electroless (chemical) deposition under an external magnetic field [5,10-16]. The chemical deposition has a great advantage because the nanoparticles with a wide variety of compositions and sizes can be obtained in a large scale.

In the present work we suggest a template synthesis of Co-Ni nanoparticles through a borohydride reduction at room temperature with  $\text{NaBH}_4$  in a mixture of water solution of the chloride salts using graphite as a support in the presence of  $\beta$ -cyclodextrine to avoid the nanoparticle aggregation and also by changing the ratio of Co:Ni to improve the magnetic properties of the Co-Ni alloyed nanomaterials.

## 2. EXPERIMENTAL SET-UP

Intermetallic Co-Ni nanoparticles are synthesized through a borohydride reduction method with 0.2M  $\text{NaBH}_4$  in a mixture of aqueous solutions of 0.1M  $\text{CoCl}_2 \cdot 6\text{H}_2\text{O}$  and 0.1M  $\text{NiCl}_2 \cdot 6\text{H}_2\text{O}$  respectively at a ratio Co:Ni = 1:1, 4:1, 1:4. To reach the ratio Co:Ni = 1:1 chosen according to the phase diagram of the binary Co-Ni system we used 25 ml 0.1M  $\text{CoCl}_2 \cdot 6\text{H}_2\text{O}$  and 25 ml 0.1M  $\text{NiCl}_2 \cdot 6\text{H}_2\text{O}$ , respectively for a ratio Co:Ni = 4:1 – 40 ml 0.1M  $\text{CoCl}_2 \cdot 6\text{H}_2\text{O}$  and 10 ml 0.1M  $\text{NiCl}_2 \cdot 6\text{H}_2\text{O}$  and for a ratio Co:Ni = 1:4 - 10 ml 0.1M  $\text{CoCl}_2 \cdot 6\text{H}_2\text{O}$  and 40 ml 0.1M  $\text{NiCl}_2 \cdot 6\text{H}_2\text{O}$ . To fully complete the reduction process in the all cases the quantity of the reducing agent stabilized with NaOH is 50 ml 0.2M  $\text{NaBH}_4$ . Citric acid ( $\text{C}_6\text{H}_8\text{O}_7$ ) is used as a stabilizing ligand. We used a quantity of 0,44g.

The synthesis is carried out in a double-wall cell to keep a constant temperature (by a thermostat) ensuring a consecutively introducing of the initial solutions and continuously mechanical stirring of the reaction mixture with a magnetic stirrer. The experiments are run at room temperature and atmospheric pressure. The reduction process is

completed in 2 minutes adding the reducing agent drop wise. Fine powder precipitates are obtained. They are filtrated, washed with a distillate water and alcohol and dried in a vacuum oven during 24 hours at 100 °C.

Intermetallic Co-Ni nanoparticles are synthesized through the same borohydride reduction method by the help of template technique using a carbon-containing support at the same technological conditions as in the case of the synthesis without using a support (the same concentrations and quantities of the reaction solutions and reducing agent solution, the same ratio Co:Ni=1:1, 4:1, and 1:4).

As a support is used a fluorinated graphite (CF) in the presence of  $\beta$ -cyclodextrin ( $\beta$ -CDx). In this way carbon-based nanocomposites are in-situ obtained. The used quantities of CF and  $\beta$ -CDx are respectively 0.36 g /100 ml. It is realized the ratio 20% CF: 20%  $\beta$ -CDx: 60% Co-Ni nanoparticles.

The morphology of the synthesized Co-Ni nanoparticles and their carbon-containing nanocomposites is investigated by the help of Scanning electron microscopy (SEM). The SEM images are made with a JEOL JSM 6400F (Japan) SEM microscope at accelerating voltage of 20 kV in three regimes: a secondary electron image (SEI image), a back reflex electron composition image (BEC image), and a split/shadow image, the so-called a combined regime (SPI image). The SEI images give information for the investigated sample surface, while the BEC images – for its chemical composition. The dark regions of the BEC images characterize the existence of atoms with a smaller atom number, while the light region brings information for an existence of atoms with bigger atom number. The elemental dispersitive analysis (EDS) is made using the same SEM microscope with an appliance for Energy-dispersive X-ray spectroscopy. The phase composition of the investigated samples is determined by X-ray diffraction (XRD). The X-ray diffraction patterns of all samples are collected within the  $2\theta$  range from 10° to 95° with a constant step 0.03° and counting time 1 s/step on Philips PW 1050 diffractometer using  $\text{CuK}\alpha$  radiation.

The magnetic behaviour of the samples based on the synthesized Co-Ni nanoparticles and their carbon-containing composites are studied by Vibrating Sample Magnetometer (VSM) in external magnetizing field at a fixed frequency of about 80 Hz at room temperature. The sample is vibrated by the vibrator at right angles to the external magnetic

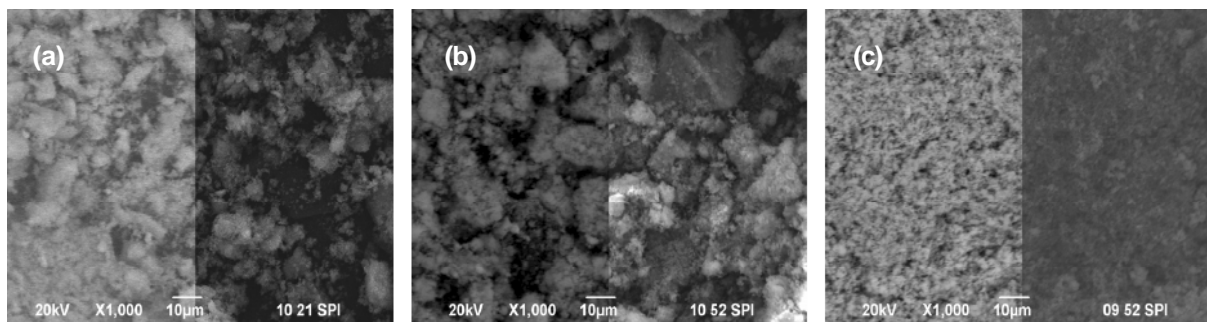


**Fig. 1.** SEM images at a magnification x1000 in SPI regime of Co-Ni nanoparticles synthesized at a different ratio: a-Co:Ni=1:1 (sample 1), b-Co:Ni=4:1 (sample 2), c-Co:Ni=1:4 (sample 3).

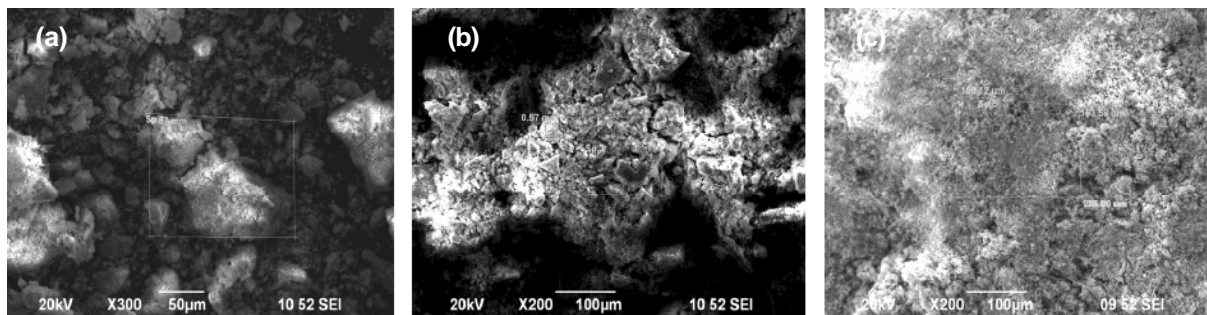


**Fig. 2.** SEM images with indicated areas where the EDS analysis is made: a- Co-Ni nanoparticles/Co:Ni=1:1 (sample 1-spectrum Sp1), magnification x300; b-Co-Ni nanoparticles/Co:Ni=4:1 (sample 2-spectrum Sp3), magnification x200; c-Co-Ni nanoparticles/ Co:Ni=1:4 (sample 3-spectrum Sp5 of), magnification x200.

field that is supplied by an electromagnet. The direction of magnetization of the sample changes in response to the applied field and thus describes a characteristic hysteresis loop. The sensitivity of the method is limited mainly by the noise mechanically transmitted from the vibrator to the pick-up coils, which is well suppressed in commercial models.

### 3. RESULTS AND DISCUSSION

#### 3.1. Investigation of the morphology of Co-Ni nanoparticles obtained at a different ratio Co: Ni. SEM results

SEM images of Co-Ni nanoparticles synthesized respectively at a ratio Co:Ni=1:1 (sample 1), Co:Ni=4:1 (sample 2) and Co:Ni=1:4 (sample 3) are shown in Fig. 1. The images are made at a magnification x1000 in SPI regime.

The SEM images show that the synthesized Co-Ni nanoparticles are too small irregular in shape. The particles are aggregated, because of unsaturated chemical bonds on nanoparticle surface and magnetic interaction forces existing between the particles. The observe aggregates are in size from 0.5 to 100 µm. Based on the SEM images it

could be said that the different Co:Ni ratio influences the morphology of the samples – it is observed some difference in the sample morphology (in a particle shape and size). But in the all cases (Co:Ni=1:1, 4:1, and 1:4) the morphology is typical for alloyed materials. As it is mentioned above the dark regions of the BEC images characterize the existence of atoms with a smaller atom number - that is Co, which atom number is 27), while the light region brings information for the existence of atoms with bigger atom number – it is Ni with atom number 28). In the case when the amount of Co is greater than the amount of Ni (the set in the initial reaction solutions ratio of Co:Ni=4:1) the morphology of the synthesized Co-Ni nanoparticles is uniform consisted from small aggregates almost the same in size. The light areas typical for the Ni content are less than dark areas characterizing the Co content.

#### 3.2. Investigation of the elemental composition of Co-Ni nanoparticles obtained at a different ratio Co: Ni. EDS results

SEM images with the indicated areas where EDS analysis is carried out of the sample 1 (Co:Ni = 1:1), sample 2 (Co:Ni = 4:1) and sample 3 (Co:Ni = 1:4) are presented in Fig. 2. The EDS spectra for the

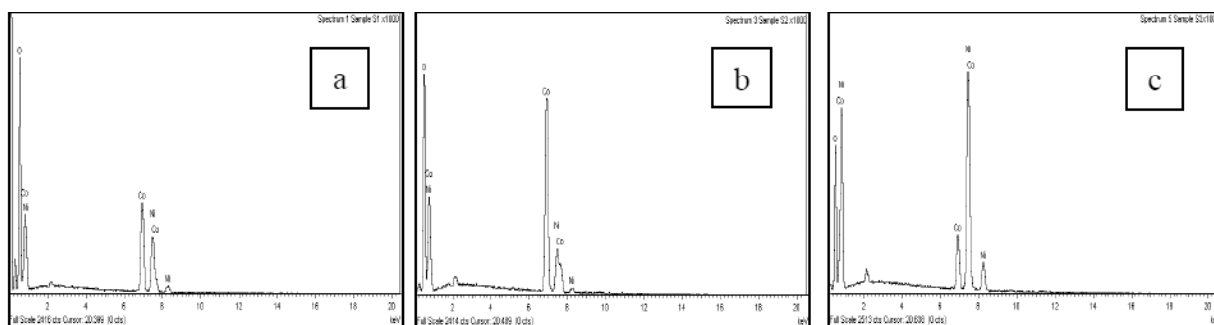


**Fig. 3.** EDS spectra for a distribution of the elements on the Co-Ni nanoparticle surface in the areas shown on the SEM images in Fig. 2; a-sample 1/Co:Ni = 1:1, spectrum Sp1; b-sample 2/Co:Ni = 4:1, spectrum Sp3, c- sample 3/ Co:Ni = 1:4, spectrum Sp5.

distribution of the Co and Ni elements on the nanoparticle surface in the indicated areas are shown in Fig. 3, while the experimental analytical data for the elemental (Co, Ni) composition of the investigated samples in the same areas are given in Table 1.

Based on the results from the EDS analysis it could be said that the ratio of Co:Ni (1:1, 4:1 and 1:4) set up in the initial reaction solutions is approximately kept in the obtained nanoparticles.

### 3.3. Investigation of the morphology of carbon-containing composites based on Co-Ni nanoparticles obtained at a different ratio Co: Ni. SEM results

SEM images of Co-Ni nanoparticles synthesized at a ratio Co:Ni=1:1 (sample 4), Co:Ni=4:1 (sample 5) and Co:Ni=1:4 (sample 6) using graphite as a support in the presence of  $\beta$ -cyclodextrin are shown in Fig. 4. The images are made at a magnification x1000 and in SPI regime.

The graphite used as a support is characterized by a flake-like structure that has influenced the

formation of the intermetallic Co-Ni nanoparticles during their synthesis. The morphology of the carbon-containing nanocomposites based on the Co-Ni nanoparticle is similar to that of the graphite: small spherical and irregular in shape particles can be seen such as the flake-like particles of the graphite. The structure of the  $\beta$ -cyclodextrin ( $\beta$ -CDx) used as a capping agent during the synthesis to prevent nanoparticles' aggregation represents hollow sphere with functional groups situated on its surface—sugar molecules bounded together in a ring (cyclic oligosaccharides creating a cone shape). It is observed in Fig. 4 that the nanoparticles are deposited among the graphite grains and surrounded

**Table 1.** Data for the elemental composition of a sample 1, 2, and 3.

Element	Sample 1 Atomic %	Sample 2 Atomic %	Sample 3 Atomic %
O K	72.20	56.34	57.35
Co K	16.35	35.26	7.49
Ni L	11.45	8.40	35.16
Totals	100	100	100

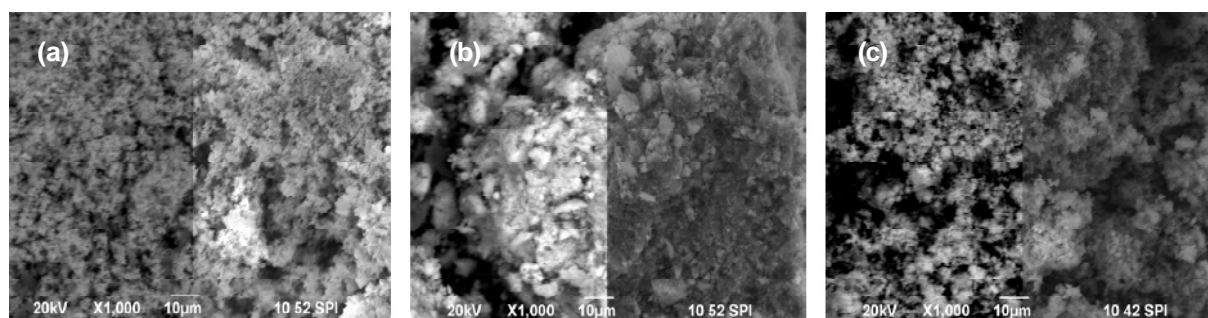


**Fig. 4.** SEM images at a magnification x1000 in SPI regime of Co-Ni nanoparticles synthesized at a different ratio Co:Ni using graphite as a support in the presence of  $\beta$ -cyclodextrin: a-sample 4/Co:Ni=1:1, b-sample 5/Co:Ni=4:1, c-sample 6, Co:Ni=1:4.

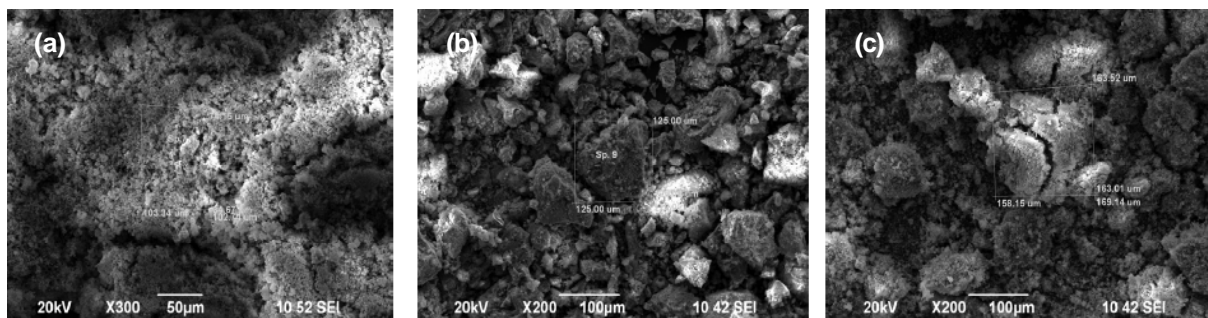


**Fig. 5.** SEM images with indicated areas where the EDS analysis is made of Co-Ni nanoparticles synthesized at a different ratio Co:Ni using graphite as a support in the presence of  $\beta$ -cyclodextrin: a- Co-Ni nanoparticles/Co:Ni=1:1 (sample 4 - spectrum Sp7), magnification x300; b- Co-Ni nanoparticles/Co:Ni=4:1 (sample 5 - spectrum Sp9), magnification x200; c- Co-Ni nanoparticles/Co:Ni=1:4 (sample 6 - spectrum Sp9), magnification x200.

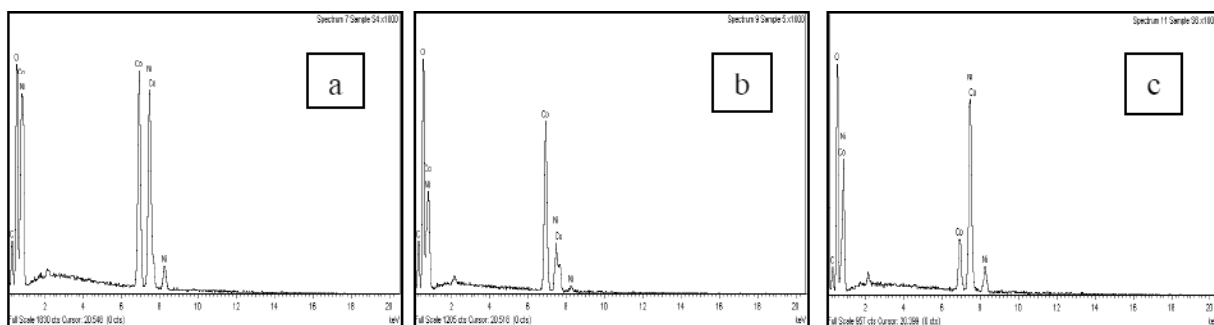


**Fig. 6.** EDS spectra for a distribution of the elements on the Co-Ni nanoparticle surface in the areas shown on the SEM images in Fig. 5: a-sample 4/Co:Ni = 1:1, spectrum Sp7; b- sample 5/Co:Ni = 4:1, spectrum Sp9; c-sample 6/Co:Ni = 1:4,spectrum Sp11.

with the  $\beta$ -CDx. It could be said that when fluorinated graphite is used as a support the morphology is typical for the morphology of the graphite itself.

It can also be seen that the ratio of Co:Ni also influences the nanoparticle formation. In this case when the Co-Ni nanoparticles are synthesized using graphite as a support in the presence of  $\beta$ -CDx during the synthesis it could be seen a light difference in the morphology of the sample 4, 5, and 6. May be it is due to graphite support that influences the nanoparticle formation. When the *Ni content* is the same (Co:Ni=1:1 and 4:1) the morphology of sample 4 and 5 distinguishes, but when the *Co content* is the same (Co:Ni=1:1 and 1:4) the morphology of the sample 4 and 6 is almost the same. The

morphology of the samples 4 and 6 is homogeneous, consisting of uniformly distributed particles of the same size, while the morphology of the samples 5 is characterized by smaller and bigger nanoparticles irregular in shape presenting nanoparticle aggregates.

### 3.4. Investigation of the elemental composition of carbon-containing composites based on Co-Ni nanoparticles obtained at a different ratio Co:Ni. EDS results

SEM images with the indicated areas where EDS analysis is carried out of the sample 4 (Co:Ni = 1:1), sample 5 (Co:Ni=4:1) and sample 6 (Co:Ni=1:4) using graphite as a support in the presence of  $\beta$ -cyclodextrin are presented in Fig. 5. The EDS spectra for the distribution of the Co and Ni elements on the nanoparticle surface in the indicated areas are shown in Fig. 6, while the elemental composition of the investigated samples in the same areas are given in Table 2.

In the case when graphite is used as a support in the presence of  $\beta$ -cyclodextrin during the

**Table 2.** Data for the elemental composition of a sample 4, 5, and 6.

Element	Sample 4 Atomic %	Sample 5 Atomic %	Sample 6 Atomic %
O K	38.77	43.14	48.91
Co K	15.00	19.63	6.72
Ni L	16.12	5.46	26.28

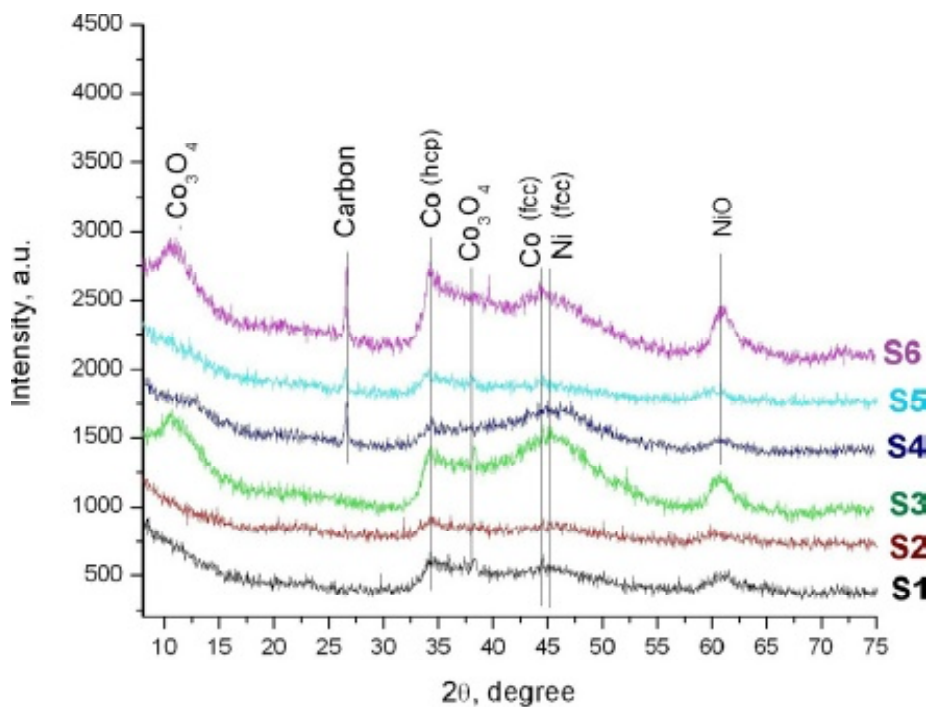


**Fig. 7.** XRD spectra of Co-Ni nanoparticles synthesized at a different ratio Co:Ni: without a support S1-Co:Ni=1:1, S2-Co:Ni=4:1, S3-Co:Ni=1:4; with a support S4-Co:Ni=1:1, S5-Co:Ni=4:1, S6 – Co:Ni=1:4.

synthesis the ratio Co:Ni=1:1, 4:1 and 1:4 set in the reaction solution is also reproduced in the Co-Ni nanoparticles.

### 3.5. Results from the XRD analysis

XRD patterns of the Co-Ni nanoparticles synthesized at a different ratio Co:Ni (respectively 1:1, 4:1 and 1:4) including when graphite is used as a support in the presence of  $\beta$ -cyclodextrin during the reduction process are compared in Fig. 7.

Since both cobalt and nickel have the same face-centered cubic (fcc) phases and their character peaks appear at almost the same diffraction angle, it is not easy to distinguish these two metals. It can be seen that all samples have the same character peak: a broad prominent peak at around  $2\theta$  value of  $45^\circ$  corresponding to both Co (fcc) and Ni (fcc) phases. The peak at around  $2\theta$  value of  $34^\circ$  describes Co hexagonal centered phase (hcp). The XRD analysis proves also the formation of oxide phases of Co and Ni. The peaks at around  $2\theta$  values of  $10^\circ$  and  $37^\circ$  are assigned to  $\text{Co}_3\text{O}_4$  phase. The peak at around  $2\theta$  of value  $62^\circ$  is related to NiO phase.

XRD spectra of the Co-Ni nanoparticles template synthesized using graphite as a support in the presence of  $\beta$ -cyclodextrin, that is to say XRD spectra of carbon-containing nanocomposites exhibit

the same peaks as in the case of the Co-Ni nanoparticles synthesized without applying a template technique. The XRD patterns prove the formation of phase of Co (fcc, hcp), Ni (fcc),  $\text{Co}_3\text{O}_4$ , and NiO at the same values of  $2\theta$ . The unique difference observed is the peak at around  $2\theta$  of value  $26^\circ$  that confirms the carbon phase due to the graphite support.

Examining the XRD patterns of the synthesized Co-Ni nanoparticles compared in Fig. 7 it could be said on the basis of the peaks intensity and their position ( $2\theta$ ) that the different ratios of Co:Ni, respectively the different Co and Ni content influence the phase formation (the peaks at  $2\theta \approx 34^\circ$  assign to Co (hcp) phase, the peaks at  $2\theta \approx 45^\circ$  refer to Co (fcc) and Ni (fcc) phases, and the peaks at  $2\theta \approx 62^\circ$  are related to NiO phase). Similar interpretation concerning the influence of the Co and Ni content on the phase composition of the prepared carbon-containing nanocomposites could be done when graphite is used as a support in the presence of  $\beta$ -cyclodextrin during the synthesis. In this case of using a graphite support the peaks characterizing the carbon phase ( $2\theta \approx 26^\circ$ ) are well expressed.

In summary, the XRD spectra of Co-Ni nanoparticles and their carbon-containing composites prove exactly that during the synthesis of Co-Ni nanoparticles at a different ratio of Co:Ni (1:1, 4:1, 1:4) and also when using a carbon-based

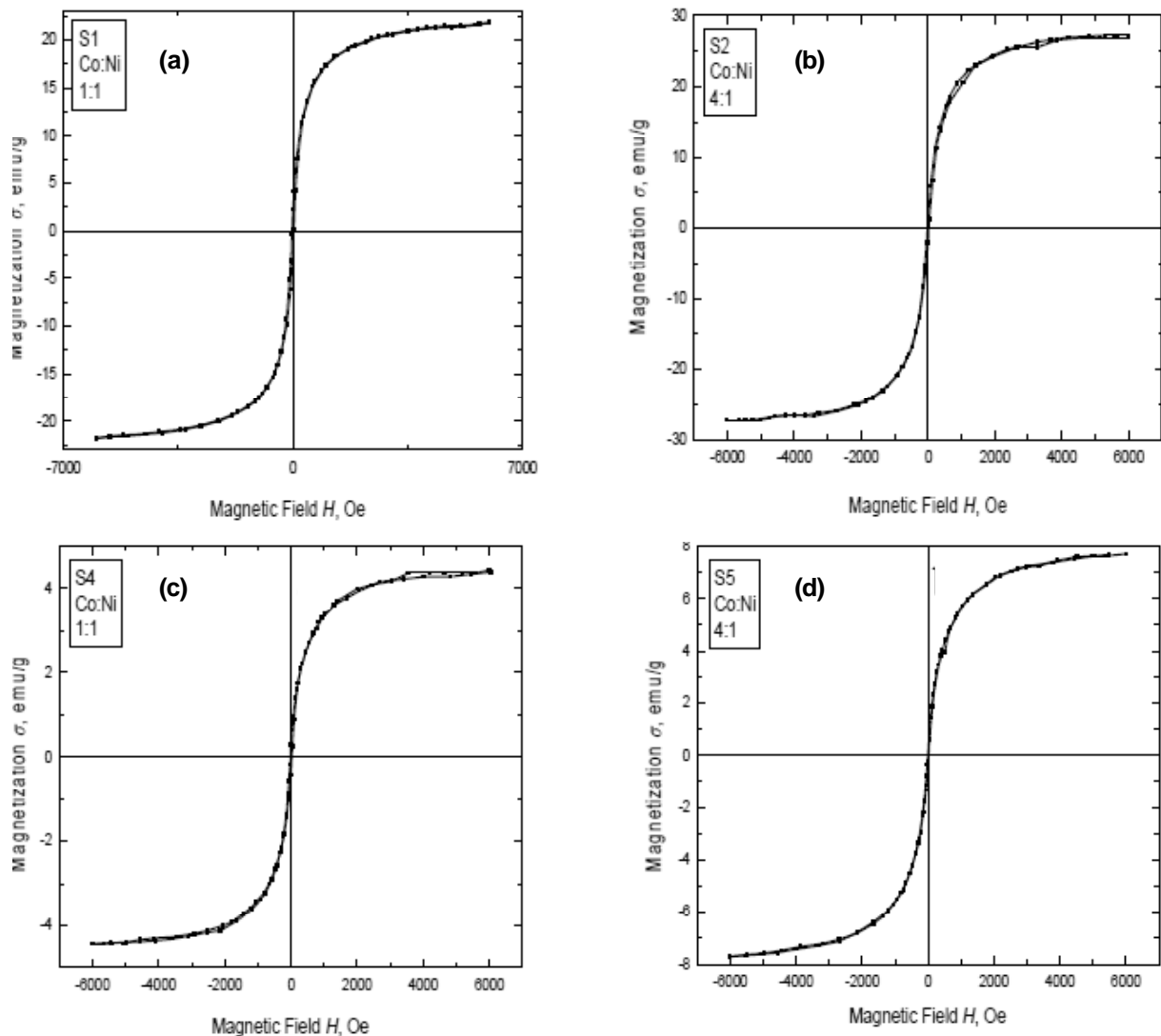


**Fig. 8.** VSM hysteresis loop measured at room temperature for the Co-Ni nanoparticles obtained at a different ratio Co:Ni including through a template synthesis using graphite as a support in the presence of  $\beta$ -cyclodextrin: a-Co:Ni=1:1 (sample 1), b-Co:Ni=4:1 (sample 2), c- Co:Ni=1:1 (sample 4), d- Co:Ni=4:1 (sample 5).

support two main phases of Co (hcp, fcc) and Ni (fcc) are formed that are in accordance with the phase diagram of the binary Co-Ni system. A phase of graphite is also detected. The observed impurity of CO,  $\text{Co}_3\text{O}_4$  and NiO phases is due to oxidizing processes.

### 3.6. Results from the measuring the magnetization of the obtained materials based on Co-Ni nanoparticles and their carbon-containing nanocomposites

The magnetic measurements of the Co-Ni nanoparticles were performed at room temperature using Vibrating Sample magnetometer (VSM). Both

the saturation magnetization,  $M_s$  [emu/g] and the coercivity,  $H_c$  [Oe] were measured in maximum magnetic field. The magnetization-magnetic field (M-H) curves (VSM hysteresis loop) of the Co-Ni nanoparticles synthesized at a different Co:Ni ratio at room temperature are shown in Fig. 8. The magnetic parameters of the samples are summarized in Table 3.

The saturation magnetization,  $M_s$  [emu/g] at room temperature of bulk pure nickel is 55 emu/g, while for the bulk pure cobalt is 161 emu/g. The values obtained in our case for the saturation magnetization of the Co-Ni nanoparticles are considerable lower than that of the bulk pure metals (Ni and Co). Probably it is due to the presence of oxides phases impurities that are not magnetic.

**Table 3.** Magnetic properties of the Co-Ni nanoparticles synthesized at a different Co:Ni ratio set up in the initial reaction solutions.

Sample	Magnetization, Ms [emu/g]	Coercivity, Hc [Oe]
S1 (Co-Ni 1:1)	21.78	26
S2 (Co-Ni 4:1)	26.55	20
S4 (Co-Ni 1:1/CF + $\beta$ -CDx)	4.42	20
S5 (Co-Ni 4:1/CF + $\beta$ -CDx)	7.7	—

According Table 3 it could be seen that the saturation magnetization, Ms [emu/g] of the Co-Ni alloy nanoparticles (sample 1 and sample 2) synthesized through a borohydride reduction increases (from 21.78 emu/g to 26.55) with increasing the concentration ratio of Co. The decrease of the observed saturation magnetization, Ms, of Co-Ni nanoparticles with respect to the bulk values (respectively 55 emu/g for nickel and 161 emu/g for cobalt) is probably due to the impurities such as CoO/Co<sub>3</sub>O<sub>4</sub> and NiO oxides.

In the case when graphite is used as a support in the presence of  $\beta$ -cyclodextrin during the template synthesis of the Co-Ni nanoparticles at ratio Co:Ni=1:1 and 4:1 (sample 4 and sample 5) the measured saturation magnetization is considerably lower than that in the case when a support is not used. It can be also seen in Table 3 that these values are considerably lower compared to these values of the bulk metals. It is due not only to the impurities of CoO and NiO, but also to the carbon and hydrogen as a result of the graphite support and  $\beta$ -cyclodextrin using during the template synthesis.

Sample 3 and sample 6 that present Co-Ni nanoparticles synthesized at room temperature at a ratio Co:Ni=1:4 respectively through a borohydride reduction and through a template synthesis using graphite as a support in the presence of  $\beta$ -cyclodextrin are manifested a very low magnetic signal and the magnetic measurements could not be performed. The bigger quantity of NiO (Co:Ni=1:4) makes worse the magnetic behavior.

The coercivity, Hc [Oe] of the Co-Ni nanoparticles in the all cases is about 20 – 26 Oe.

In summary, it could be said that based on the saturation magnetization (Ms) the Co-Ni nanoparticles synthesized at ratio Co:Ni=1:1 and 4:1 have better magnetic characteristics than that in the case of a ratio Co:Ni=1:4 and also when both

graphite support in the presence of  $\beta$ -cyclodextrin are used.

Co-Ni nanoparticles (Co:Ni=1:1 and 4:1) have soft ferromagnetic behavior. Their magnetic properties are appropriate for biomedical applications as diagnostic tools and targeting treatment in cancer and other diseases. The magnetic properties obtained for the Co-Ni nanoparticles answer to magnetic field strengths required to manipulate nanoparticles to have no harmful effect on the biological tissue. Co-Ni nanoparticles have a ferromagnetic behavior that magnetizing strongly under an applied field, but retaining no permanent magnetism once the field is removed.

## 4. CONCLUSION

Template synthesis through a borohydride reduction using carbon-containing support (graphite CF and  $\beta$ -cyclodextrin) proves to be an effective way to obtain *in situ* new carbon based composites with active intermetallic Co-Ni nanoparticles exhibiting magnetic behavior appropriate for biomedical applications because of their magnetic properties. Prepared are fine Co-Ni powders, which have morphology typical for alloys and also magnetic properties to be used successfully in biomedicine.

CF matrix is suitable in terms of obtaining fine monodispersed nanoparticles with great size distribution. The particles are over 100 nm in size. They have irregular shape and tend to aggregate spontaneously. Aggregates ranging from 0.5 to 100  $\mu$ m are observed. To avoid that  $\beta$ -cyclodextrin is used as capping agent. X-ray diffraction analysis of Co-Ni particles and their carbon-based composites with a matrix of graphite has proved that at used mass ratios of Co:Sn=1:1, 4:1 and 1:4, set in the reaction solutions two main phases of Co and Ni are formed. This is in accordance with the phase diagrams of the Co-Ni binary systems. SEM studies of the samples based on the synthesized intermetallic nanoparticles with graphite matrix and the use of  $\beta$ -cyclodextrin show a homogeneous and dense morphology.

This shape is similar to the shape of the substrate (graphite). SEM images of the synthesized Co-Ni particles show that in a case of using graphite as a matrix in the presence of  $\beta$ -cyclodextrin the morphology is characterized by flake-shape particles. This morphology is typical for the morphology of the graphite itself.

Co-Ni nanoparticles synthesized at ratios of Co:Ni=1:1 and 4:1 have soft ferromagnetic behavior that magnetizing strongly under the external applied

field, but retaining no permanent magnetism once the field is removed. The saturation magnetization,  $M_s$  [emu/g] of the Co-Ni alloyed nanoparticles (sample 1 and sample 2) synthesized through a borohydride reduction increases (from 21.78 emu/g to 26.55) with increasing the concentration ratio of Co. Their magnetic properties are appropriate for biomedical applications as diagnostic tools and targeting treatment in cancer and other diseases.

## ACKNOWLEDGEMENTS

The authors acknowledge the financial support for this investigation provided by the National Science Fund at the Ministry of Education and Science – Bulgaria under the Contract DN 07/29–16.12.2016 (respectively under the Contract No 881/10.01.2017 of the Scientific Research Center at the UCTM-Sofia).

## REFERENCES

- [1] R. Brayner, M.-J. Vaulay, F. Fievet and T. Coradin // *Chem. Mater.* **14** (2002) 1190.
- [2] M. Vazquez, C. Luna, M.P. Morales, R. Sanz, C.J. Serna, C. Mijangos, M. del Puerto Morales, C.J. Serna and M. Vázquez // *Nanotechnology* **14** (2003) 268.
- [3] J. Neamtu, I. Jitaru, T. Malaeru, G. Georgescu, W. Kappel and V.V. Alecu // *NST Nanotech* **1** (2005) 222.
- [4] J. Park, E. Kang, S.U. Son, H.M. Park, M.K. Lee, J. Kim, K.W. Kim, H.-J. Noh, J.-H. Park, C.J. Bae, J.-G. Park and T. Hyeon // *Adv. Mater.* **17** (2005) 429.
- [5] C. Yu and J.S. Qiu // *Chemical Engineering Research* **86** (2008) 904.
- [6] Ming Jun Hu, Bin Lin and Shu Hong Yu // *Nanoresearch* **1** (2008) 303.
- [7] S. Sharma, N.S. Gajbhiye and R.S. Ningthoujam // *J. of Colloid and Interface Science* **351** (2010) 323.
- [8] Neamtu and N. Verga // *J. of Nanomaterials and Biostructures* **6** (2011) 969.
- [9] M. Kawamori, Shunsuke Yagi and Eiichiro Matsubara // *J. of the Electrochemical Society* **159** (2011) E37.
- [10] M. Kawamori, S. Yagi and E. Matsubara // *J. of the Electrochemical Society* **159** (2012) E37.
- [11] Matti M. van Schooneveld, Carlos Campos-Cuerva, Jeroen Pet, Johannes D. Meeldijk, Jos van Rijssel, Andries Meijerink, Ben H. Erne and Frank M. F. de Groot // *J. Nanopart. Res.* **14** (2012) 991.
- [12] Rakkiyasamy Manimekalai, Kalimuthu Kalpanadevi and Rangasamy Sinduja // *Research Journal of Chemical Sciences* **3** (2013) 76.
- [13] Wanheng Lu, Hongying Yu, Dongbai Sum and Lixiang Lu // *J. Nanoengineering and Nanosystems* **228** (2014) 52.
- [14] S. A. Salman, T. Usami, K. Kuroda and M. Okido // *J. of Nanotechnology* **6** (2014) 193.
- [15] Mai Woon Lee, Muhammad Aniq Shazni Mohammad Haniff, Aun Shih Teh, Daniel C.S. Bien and Soo Kien Chen // *J. of Experimental Nanoscience* **10** (2015) 1232.
- [16] Jiaqiang Huang, Biao Zhang, Yu Yang Xie, Wilson Wei King Lye, Zheng-Long Xu, Sara Abouali, Mohammad Akbari Garakani, Jian-Qiu Huang, Tong-Yi Zhang, Baoling Huang and Jang-Kyo Kim // *Carbon* **100** (2016) 329.